

STUDY ON DROP SIZE DISTRIBUTIONS OF EVAPORATING WATER AND SALINE SPRAYS

H.J. Holterman, A.A. Pronk

Wageningen UR – Plant Research International
P.O. Box 616; 6700 AP Wageningen; The Netherlands

Key words: PDA, sprays, dust emission, evaporation, spectral distribution, pollution

Summary

In order to mimic fine dust as emitted from stables, to be used in field experiments, a fine spray of a suspension of a non-volatile tracer material was released upwind from the dust measuring site. The distance between sprayer and measuring site must be large enough to allow all water solvent to evaporate before the particles would reach the measuring site. In the current preliminary study the drying process and the particle size distributions were investigated under various climatic conditions. Adding salt to the spray liquid may affect the hygroscopic nature of the particles, which subsequently may affect the size of the particles. Drop size distributions of several sprays at various downwind distances were measured using a PDA technique (Aerometrics/TSI). Drops with very fine spray quality ($D_{V50} \sim 69 \mu\text{m}$) were produced using a high speed rotary atomizer. Additionally, a physical model for evaporating sprays was developed to simulate these experiments.

The results showed that both water and saline sprays evaporated in a similar way, depending on ambient temperature (T) and relative humidity (RH). Drop size distributions from measurements and simulations agreed fairly well. With the saline sprays a considerable amount of small drops ($<10 \mu\text{m}$) remained, indicating that small saline drops remain (partially) hydrated, depending on T and RH. This was supported by the model results, showing that solvent evaporation rates for concentrated saline drops may be considerably reduced.

Introduction

In livestock breeding, dust emissions (typical size 5-10 μm) from stables cause considerable environmental pollution. Air quality may be improved by placing trees around these stables. However, there is only little experimental evidence for a quantitative assessment of the dust filtering effect of trees surrounding a stable. Therefore field experiments were planned to investigate this filtering effect of trees on passing dust clouds. These experiments require the availability of (artificial) dust particles of known size distributions in sufficiently large quantities. Using a spray application technique, droplets of a well-known size distribution can be produced. Subsequently, with a known solute concentration in the spray liquid, the final particle size distribution after complete evaporation of the solvent (water) can be estimated easily. Obviously, the spray drops need to dry in air before reaching the trees where the

filtering effect is to be measured. The rate of drying and the average wind speed determine the minimal upwind distance required for droplet release.

The current study deals with the actual drying process and the particle size distributions under various climatic conditions. Real dust may be dry or hydrated depending on its hygroscopic nature. Therefore salt was added to the spray liquid which may affect the hygroscopic nature of the particles, and consequently, the drying process. This may affect both the size distribution and the retention of impacting particles. In order to quantify the evaporative process and the final particle size distributions for the dust-like particles, drop size distributions of water and saline sprays at various downwind distances were measured using a PDA technique. Additionally, a physical transport model for evaporating sprays was developed to simulate these experiments.

Materials & methods

The equipment used is a one-dimensional Phase-Doppler Particle Analyzer (PDPA; Aerometrics, USA), connected to photo-detection module PDM1000 and size analysis hardware FSA3500 (TSI, USA), and using FlowSizer software (TSI, USA) for data acquisition and analysis. The light source is a 1 W Argon-ion laser (Lexel 85-1), of which only the green light (514.5 nm) is used. The optical transmitter and receiver are positioned in the 40° forward scattering setup, with 500 mm front lenses, in such a way that the principal measuring direction of particle flow is horizontal. The transmitter was equipped with a beam expander, so that the range of detectable diameter was 0.9 through 301 μm .

All experiments were done with rotary disc atomizers, Turbair Electrafan 240 (Micron Sprayers Ltd., UK). Typical rotational frequency is 10^4 rpm; diameter of the toothed rotary disc is 0.09 m. The atomizer is supplied with a ventilator (diameter 0.25 m) which thrusts the spray cloud forward. Six atomizers were available. Two spray liquid were used: tap water and tap water with 10 g/L table salt (NaCl). Solubility in water is 360 g/L for the range of temperatures used, approximately (CRC, 1977). To affect the evaporation rate of the water solvent, the spray chamber was controlled at three pairs of temperature and relative humidity: 15°C / 80%, 20°C / 60% and 25°C / 40%.

The setup of the atomizer and the PDA is shown in Fig. 1. The electromotor of the atomizer drives both the fan and the atomizer disc. The fan supplies a forward thrust of air to move the droplets created by the toothed atomizer disc towards the plane of measurement. The spray chamber size is 15x5.5x3.5 m (LxWxH) and the equipment was located in the central part to avoid interference of the spray cloud with the chamber walls. The flow axis was about 1 m above the ground. PDA transmitter and detector were fully shielded with plastic foils to prevent contamination with spray droplets. Distance between atomizer and PDA was set to 1, 2, 3, 4, 5 and 7 m.

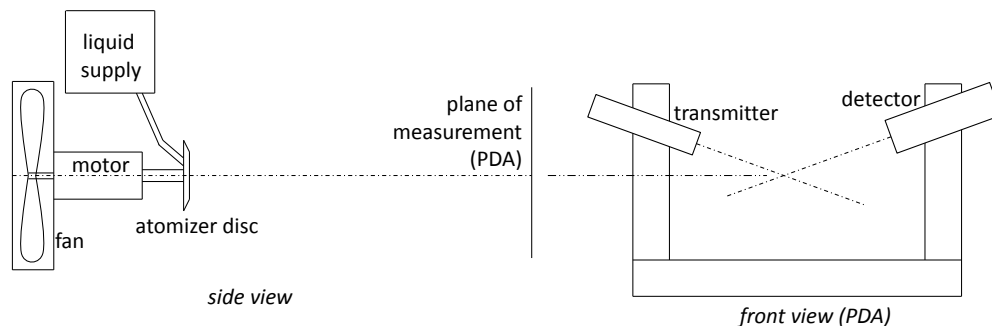


Fig. 1. Schematic layout of experimental setup. Side view on left-hand side, front view on right-hand side. The atomizer axis is lined up with the PDA cross-section area. Distance between atomizer and plane of measurement can be adjusted.

Measurements

Initial drop size distributions were obtained by setting a relatively short distance (1 m) between atomizer and PDA together with a relatively cold and humid chamber climate (temperature 15°C and relative humidity 80%). In this setup, travelling times of droplets were very short with respect to the evaporation times and evaporation effects could be neglected. Fig. 2 shows the averaged initial drop size distribution by volume. Characteristic parameters: D_{V10} 40 μm , D_{V50} 69 μm , D_{V90} 105 μm .

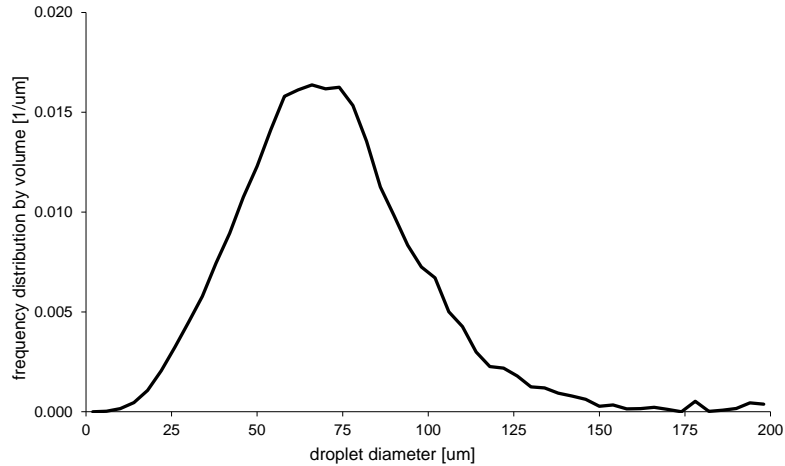


Fig. 2. Initial drop size distribution (by volume) of the Turbair Electrafan 240. Average over six atomizers, measured at the flow axis, 1 m from the atomizer disc. Tap water; T:15°C; RH:80%.

The measurements indicate that the average velocity (v) as a function of distance from the atomizer (x) appears to follow the next empirical relation well (Fig. 3.a):

$$v = b_0 e^{-b_1 x} \quad (1)$$

where $b_0 = 6.35 \text{ m}\cdot\text{s}^{-1}$ and $b_1 = 0.241 \text{ m}^{-1}$ are empirical constants.

As a rule of thumb, measurements should involve the collection of 10^4 drops for a reasonable spectral analysis (Holterman, 2000). However, particularly at larger distances collecting this number of drops was not feasible within a reasonable measuring time (<1 hour). The lowest number of drop counts was 500 for a tap water spray at distance 7 m under warm/dry conditions.

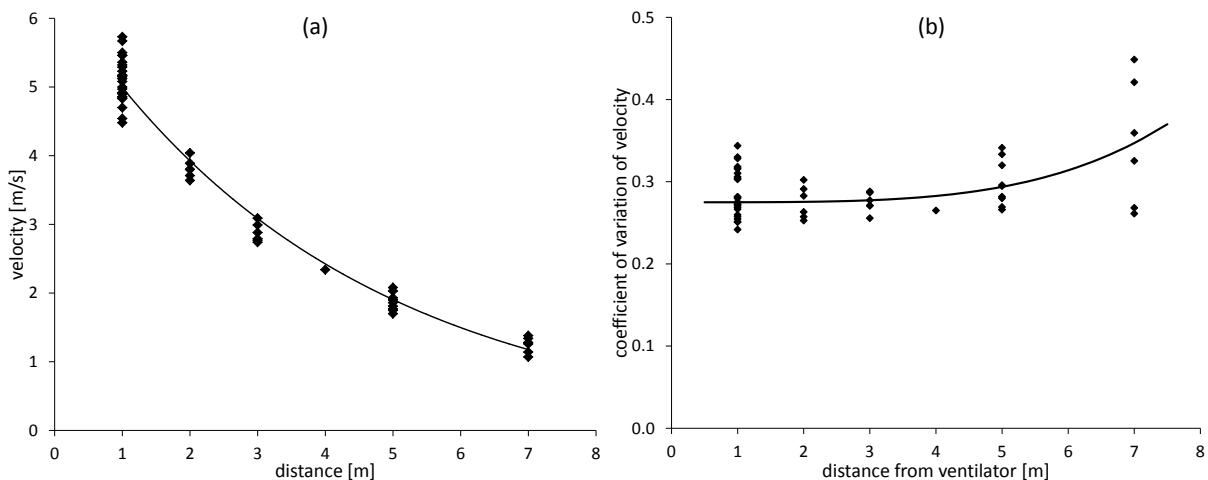


Fig. 3. Average velocity (a) and its coefficient of variation (b) of spray drops as a function of distance from the atomizer. Dots: measurement results; solid lines: fitted curves.

Fig. 3.b shows the coefficient of variation (CV) in the measured droplet velocities for all experiments, as a function of distance. The solid line is an empirical fit, indicating that CV is almost constant for the distances considered, though there is a slight tendency to increased CV at larger distances. However, the uncertainty is relatively large there due to the low droplet counts at larger distances. The spreading at $x = 1$ m seems large as well, but it merely reflects the larger number of measurements at this distance. CV as a function of x is fitted well by the following equation:

$$CV(x) = \alpha_0 + \alpha_1 x^4 \quad (2)$$

with $\alpha_0 = 0.275$ and $\alpha_1 = 0.00003$.

The measured drop size distributions of water and saline sprays at various downwind distances are shown in Fig. 4. The distributions with water seem to indicate that the size spectra do not change much with distance. However, it may well be that the spray evaporates in such a way that effectively the drop size spectrum remains almost the same, at least for a while. The increased uncertainty for larger distances is due to the lower number of droplets measured. On the other hand, the drop size spectra for the saline spray clearly show a shift towards small droplets. Apparently, the hygroscopic nature of the salt prevents the water solvent from complete evaporation, thus leaving small hydrated particles behind. Similarly, the water sprays at 5 m and 7 m seem to produce some tiny droplets as well ($<5 \mu\text{m}$), which may be due to hygroscopic impurities in the tap water.

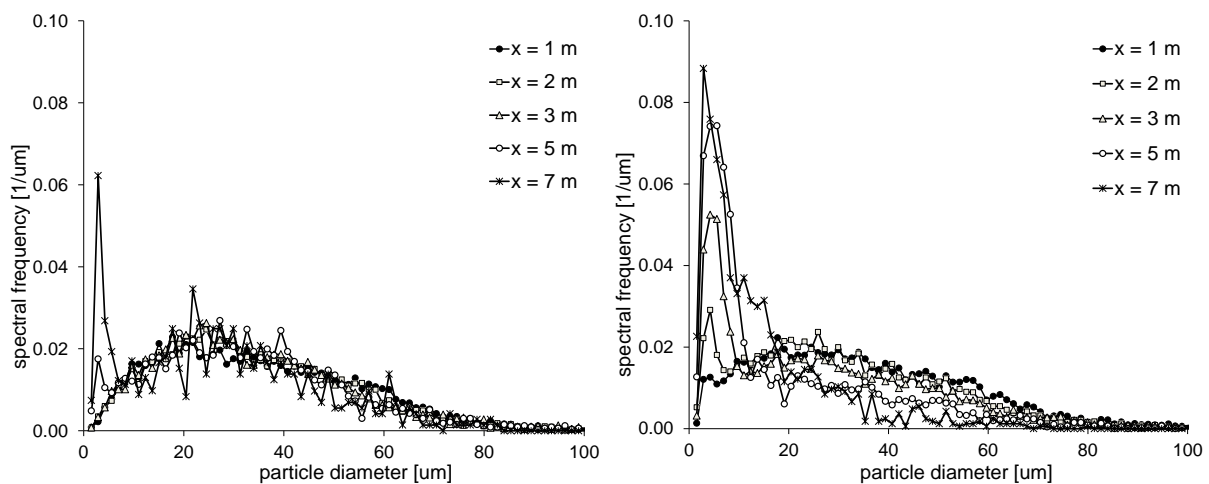


Fig. 4. Drop size distributions (by number) for water sprays (left) and saline sprays (right) measured at several distances from the atomizer. Temperature 25°C; relative humidity 40%.

Fig. 5 shows the measured data rate in the various situations as a function of distance from atomizer to PDA. Data rate reduces rapidly with increasing distance, which can only be partly explained by the dilution of the expanding spray cloud with distance. Evaporation of the smaller droplets causes loss of particles in the cloud, which gives rise to a considerable reduction in data rate. This is supported by the observation that with increasing distance the measured data rates appear to be higher for saline sprays than for water sprays. As mentioned above, due to their hygroscopic nature small saline drops tend to live longer than small water drops. Data rates are higher under relatively cold/wet conditions compared to those under warm/dry conditions, for both water and saline sprays.

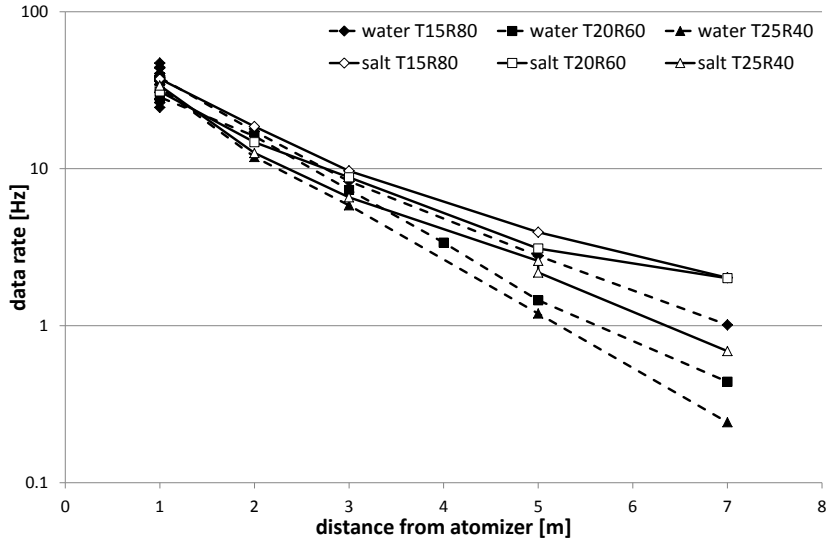


Fig. 5. Measured PDA data rates as a function of distance from the atomizer for water sprays (black symbols, dashed lines) and saline sprays (white symbols, solid lines) at different temperatures and relative humidities.

Droplet transport model

A numerical 3D model is developed to describe the flow of particles from the atomizer to the PDA measuring area. The droplet position vector \vec{x}_k at time $t_k (= k\Delta t)$ is described by the following first order relation:

$$\vec{x}_k = \vec{x}_{k-1} + \vec{u}_{k-1} \Delta t \quad (3)$$

where index $k-1$ indicates the values at the previous time t_{k-1} ; \vec{u} is the velocity of the drop. Since the drops produced by the atomizer are relatively small, the drops adapt quickly to the surrounding air. Therefore, for simplicity it is assumed that at all times the droplet velocity equals the local air velocity. So droplet velocity \vec{u} is given by the sum of average air velocity and a local turbulence velocity. Since drops will slowly settle down due to gravity, a sedimentation velocity was added as well. This yields the following droplet velocity:

$$\vec{u}_k = \vec{v}_k + \vec{r}_k + \vec{v}_{sed,k} \quad (4)$$

where \vec{v}_k is average air velocity, \vec{r}_k is turbulence air velocity and $\vec{v}_{sed,k}$ is the sedimentation velocity (which is directed vertically downward and a function of droplet diameter; Holterman, 2003), all at the current location of the droplet.

Assume the air flow from the ventilator has cylindrical symmetry, and average velocity decays exponentially with radial distance r (following a 2D Gaussian shape). Then Eq.(1) becomes:

$$v(x, r) = b_0 e^{-b_1 x} e^{-r^2/2\sigma_x^2} \quad (5)$$

where σ_x is a measure of the width of the air flow and is a function on distance. Air mass conservation requires that the total mass flow (or volume flow when neglecting air compression) of air is constant, that is, independent of distance x . This results in the following relation for σ_x :

$$\sigma_x = \sqrt{\frac{\Phi}{2\pi b_0}} \cdot e^{b_1 x/2} \quad (6)$$

where Φ is the volume flow rate of air. For a ventilator diameter of 0.25 m and air velocity $v = b_0$ near the ventilator, $\Phi = 0.31 \text{ m}^3/\text{s}$, typically. Then, at $x = 0$, $\sigma_0 = 0.09 \text{ m}$ which seems reasonable. These considerations implicitly assume that \vec{v}_k has a non-zero x component only; y and z components are assumed zero.

Air turbulence velocity is assumed to depend on its own history but it will change over time gradually and randomly:

$$\vec{r}_k = R \vec{r}_{k-1} + \gamma_k \vec{s}_k \quad (7)$$

where R is a 'memory factor' (having a value between 0 and 1) relating the current turbulence to its previous value; \vec{s}_k is a random 3D vector with components taken from the standard normal distribution and γ_k is a scalar representing the strength of the random term. A useful representation of R is given by:

$$R = e^{-\beta \Delta t} \quad (8)$$

where β is a constant to be estimated empirically. Setting $\beta = 10$ turned out to be convenient with respect to the model results. The above equation shows that the memory fades when the time interval Δt increases.

Since the turbulence velocity is the only stochastic term in Eq.(4), the variance of droplet velocity equals the variance of turbulence velocity (σ_r^2). Since in reality turbulence is present already at $t=0$, in the model a non-zero variance of turbulence $\sigma_{r,0}^2$ at $t=0$ (i.e. $x=0$) must be set. This variance can be determined from of average air velocity $v(0)$ and $CV(0)$ using Eqs.(1) and (2):

$$\sigma_{r,0}^2 = \alpha_0^2 b_0^2 \quad (9)$$

Now the first turbulence vector \vec{r}_0 is non-zero and randomly taken from a 3D normal distribution with variance $\sigma_{r,0}^2$.

Although in Eq.(7) the turbulence strength γ_k is related to time index k, from a physical point of view it seems more appropriate to relate γ_k to position vector \vec{x}_k rather than to time t_k . The following expression conveniently describes the strength of the random turbulence term as a function of position (and implicitly, through R , of time step Δt):

$$\gamma^2(x, r) = \alpha_0^2 \cdot v^2(x, r) \cdot (1 - R^2) \cdot e^{f(x)} \quad (10)$$

where $f(x)$ is an empirical function of distance, to be determined such that CV of droplet velocity at the PDA measurement location follows the observed behaviour of Fig. 3.b and Eq.(2). Simulations indicated that the following expression fits our purpose well at the distance range 1–8 m:

$$f(x) = c_0 + c_1 x + c_2 x^2 + c_3 x^3 \quad (11)$$

Where $c_0 = 0.2$, $c_1 = 0$, $c_2 = -0.02$ and $c_3 = 0.005$. For the larger distances from the atomizer, the rotating disc can be modelled as a point source where drops with zero initial velocity are released into the air stream produced by the ventilator. However, for the smaller distances this point source approximation cannot be used. In fact the drops escape from the edge of the rotating disc at high tangential speed equal to the rotational speed at the edge (typically $\sim 50 \text{ m/s}$). The drops will slow down rapidly and effectively travel their 'stopping distance' until their tangential speed is almost zero. Therefore, a more appropriate droplet source is a set of circular sources for the different drop size classes, the circles having a radius equivalent to the stopping distance for each drop size class. Stopping distance is a function of droplet diameter and is computed iteratively using the theory given by Holterman, 2003. While moving through air the droplet will become smaller due to evaporation of the water solvent. The rate of decrease of droplet diameter is given by (Holterman, 2003):

$$\frac{dD}{dt} = -\frac{p}{D} (1 + q\sqrt{Dv_{rel}}) \quad (12)$$

where D is droplet diameter, v_{rel} is the velocity of the droplet relative to the surrounding air, and p and q are constants depending on temperature, relative humidity and physical properties of water. Essentially, droplet velocity differs from local air velocity only by its sedimentation velocity, so $v_{rel} = v_{sed}$. While the droplet size decreases gradually, the salt concentration increases. Eventually, if the droplet has not deposited somewhere, the salt concentration must reach saturation. Further evaporation of water will cause the salt to crystallize inside the droplet, which makes detection using PDA in refraction mode more difficult. The consequences of this effect will be discussed later. The hygroscopic nature of saline drops reflects a reduces evaporation rate when salt concentration increases. This is accounted for in the model by scaling the parameter p linearly with volume fraction of water in the droplet.

Results

Fig. 6 shows the measured data rates for water and saline sprays for 20°C and 60% RH (also given in Fig. 5), together with results from simulations. Data rates from the simulations are relative values only, so these were scaled to fit the measured data rates at $x = 1$ m. The results indicated as model#1 represent the data rates when all drops are accounted for, including those with salt concentration above saturation and those dried completely. For model#2 the particles with salt concentration above saturation were excluded. In both cases the particles $<0.9 \mu\text{m}$ were excluded (i.e. below the detection limit of the PDA). Note that the measured curve for the saline spray is between these two model curves. This suggests that part of the smallest drops may become undetectable due to crystallization of salt, but also that some of these drops tend to withhold the water from evaporation much longer than expected. The model curve for water sprays (not shown) appeared to be essentially equal to the curve of saline/model#2.

As an example, Fig. 7 shows measured and modelled drop size distributions for a water and saline spray at distance of 3 m, temperature 25°C and relative humidity 40%. For water the measured and modelled distributions agree well. The measured spray seems to be slightly finer than the modelled spray, however the number of drops in the measured spray is relatively low ($N=5000$), so the observed distribution may not be very accurate.

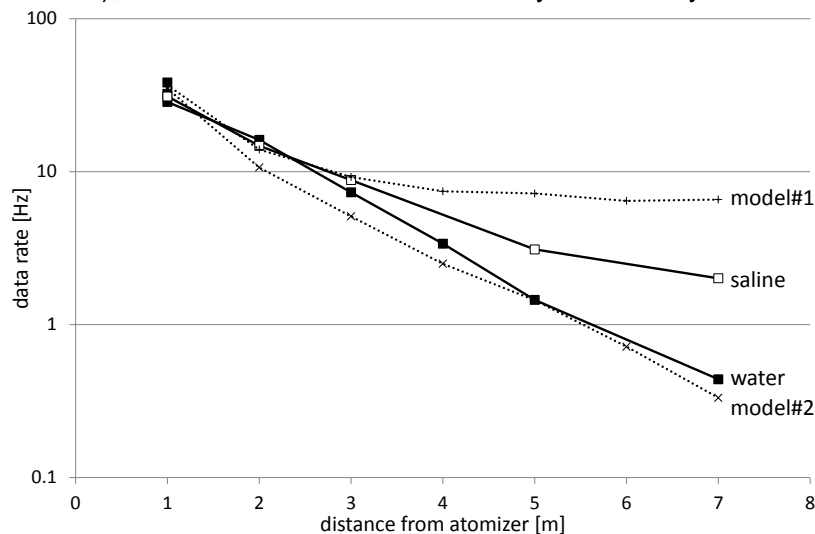


Fig. 6. Data rates for water and saline sprays as a function of distance from the atomizer ($T:20^{\circ}\text{C}$, $\text{RH}:60\%$). Solid lines: measured with PDA, dashed lines: model computations. Model#1, model#2: saline, including and excluding drops with salt concentration above saturation, respectively (see text).

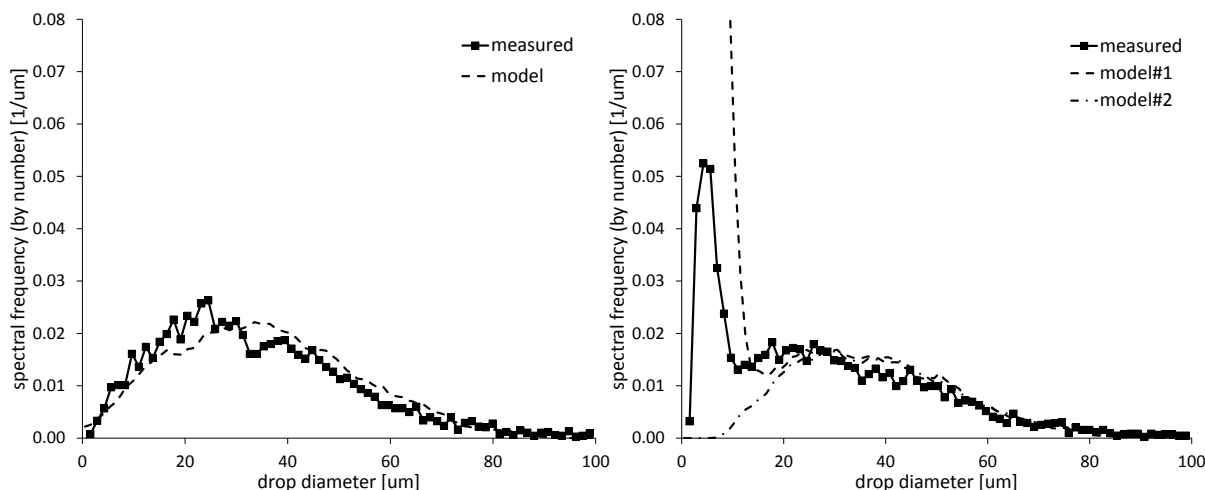


Fig. 7. Spectral frequency distribution of drop sizes. Solid line/dots: measured with PDA; dashed lines: model results. Left: water spray; right: saline spray. For saline spray the model was run including and excluding supersaturated drops (model#1 and model#2 respectively) ($T:25^{\circ}\text{C}$, $\text{RH}:40\%$, $X=3\text{m}$).

For the saline spray the spectra are similar for drops $>15\ \mu\text{m}$ and small differences may well be due to the uncertainty of the measured spectrum ($N=5600$). Below $15\ \mu\text{m}$ the two model curves separate from each other, whereas the measured curve roughly is somewhere in between. Again, this supports the idea that some small drops may be undetected due to recrystallization, while evaporation rate seems to be reduced due to hygroscopic effects.

Conclusion

The measurements of drop size distributions in this study indicated that both water and saline sprays evaporated in a similar way, depending on ambient temperature (T) and relative humidity (RH). However, with the saline sprays a considerable amount of small drops ($<10\ \mu\text{m}$) remained, indicating that small saline drops remain (partially) hydrated. The fact that such small particles were detected by PDA, which in refraction mode can only 'see' transparent drops, indicates that the evaporation rate for these concentrated saline drops is reduced considerably, most likely due to hygroscopic effects. For the water sprays tested the drop size distributions do not change much due to evaporation, as evaporated smaller drops are replaced by decreased larger ones. Although the spray transport model has a lot of assumptions with respect to the air flow generated by the ventilator, measured drop size distributions could be simulated fairly well by the spray evaporation model. However, the implementation of hygroscopic effects on evaporation rates needs further attention.

References

- Holterman, H.J., 2000: "Statistical aspects of sampling agricultural sprays", Proceedings of the 16th Annual Conference on Liquid Atomization and Spray Systems (ILASS), 11-13 Sep 2000, Darmstadt, Germany; V.4.1-6.
- Holterman, H.J., 2003: "Kinetics and evaporation of water drops in air", Report 2003-12, IMAG Wageningen, The Netherlands, 67 pp.
- CRC Handbook of Chemistry and Physics, 58th Edition, 1977. Ed. R.C. Weast. CRC Press, Cleveland OH, USA.